doi:10.1111/j.1365-2591.2006.01164.x

Changes in compaction stress distributions in roots resulting from canal preparation

A. Versluis[1], H. H. Messer[2] & M. R. Pintado[1]

[1]Minnesota Dental Research Center for Biomaterials and Biomechanics, School of Dentistry, University of Minnesota, Minneapolis, MN, USA; and [2]School of Dental Science, University of Melbourne, Melbourne, Australia

Abstract

Versluis A, Messer HH, Pintado MR. Changes in compaction stress distributions in roots resulting from canal preparation. *International Endodontic Journal*, **39**, 931–939, 2006.

Aim To examine if canal enlargement with instruments of controlled taper leads to more uniform stress distributions within a root, thereby reducing fracture susceptibility.

Methodology Finite element models of a mandibular incisor were constructed with round and oval canal profiles, based on measurements from extracted teeth. The shapes of rotary nickel–titanium instruments (ProTaper F1, F2, and F3 and ProFile size 30, 0.04 taper and size 30, 0.06 taper; Dentsply Maillefer) were superimposed on the canals. Equivalent stresses and circumferential stresses in the root were calculated for a compaction load.

Results The highest stresses were found at the canal wall. Round canals showed lower uniform distributions, whilst oval canals showed uneven distributions with high concentrations at the buccal and lingual canal extensions and greater stresses in the coronal and middle thirds than in the apical third. Preparation of round canals introduced only small circumferential stress increases in the apical half; preparation of oval canals produced substantial reductions where the canal was enlarged to a smooth round shape. Even where fins were not completely eliminated, the maximum stresses were still reduced by up to 15%. External distal and mesial surfaces of roots with oval canals showed moderate stress concentrations that were minimally affected by preparations, whilst stress concentrations emerged on roots with round canals when preparation sizes increased.

Conclusions The potential for reducing fracture susceptibility exists as a result of round canal profiles achieved and smooth canal taper. Even when fins were not contacted by the instrument, stresses within the root were lower and more evenly distributed than before preparation.

Keywords: finite element analysis, fracture resistance, nickel–titanium, root canal preparation, stress distribution.

Received 20 April 2006; accepted 15 May 2006

Introduction

Although vertical root fracture of endodontic origin is an infrequent event, the consequent tooth loss makes it a significant clinical concern (Caplan & Weintraub 1997, Fuss *et al.* 1999). Factors predisposing to vertical root fracture have been investigated using a variety of experimental approaches and are now reasonably well understood (Lindauer *et al.* 1989, Sedgley & Messer 1992, Wilcox *et al.* 1997, Lertchirakarn *et al.* 1999). Whilst many variables are outside the control of the clinician (natural root morphology, canal shape and size, dentine thickness), other factors can be addressed during treatment to reduce fracture susceptibility. These factors include final canal shape, extent of canal enlargement, and elimination of irregularities that serve as sites of stress concentration (Sathorn *et al.* 2005a).

The advent of rotary nickel–titanium instruments has led to the possibility of rounder canal profiles and

Correspondence: Antheunis Versluis, Minnesota Dental Research Center for Biomaterials and Biomechanics, School of Dentistry, University of Minnesota, 16-212 Moos Tower, 515 Delaware Street SE, Minneapolis, MN 55455, USA (Tel.: +1 612 626 3962; fax: +1 612 626 1484; e-mail: antheun@umn.edu).

more controlled taper than with hand files, and larger apical preparations have also been recommended (Glosson *et al.* 1995, Thompson & Dummer 1997, Bryant *et al.* 1998). Complete planing of canal walls and hence a completely smooth canal shape and taper remains an elusive ideal (Peters 2004). Nonetheless, elimination of irregularities in the canal wall and creation of a smooth, round canal shape throughout the length of the canal should result in a more uniform stress distribution and lower overall stresses (Sathorn *et al.* 2005a). In association with a potential strengthening of roots via adhesive root filling materials (Cobankara *et al.* 2002, Teixeira *et al.* 2004), it is not unreasonable to ask the question: Can round, smoothly tapered canal preparations potentially reduce fracture susceptibility of root-filled teeth?

Oval-shaped root canals, which are found in approximately 25% of roots (Wu *et al.* 2000), pose problems with regard both to the effectiveness of canal preparation and to fracture susceptibility. The narrow radius of curvature at the buccal and lingual extensions of the canal means that these locations serve as sites of stress concentration (Sathorn *et al.* 2005b). A prepared canal that eliminates these narrow extensions will have a more uniform stress distribution and potentially a much reduced susceptibility to fracture. However, several experimental studies using extracted teeth have demonstrated; however, that the highly flexible nickel–titanium rotary instruments tend to create a bulge in the middle part of the canal, leaving the buccal and lingual extensions largely untouched (Rödig *et al.* 2002, Weiger *et al.* 2002). Careful circumferential preparation with hand instruments (Hedstrom files), Gates Glidden burs or a specially designed device (AET) have been advocated to achieve more complete planing of the canal wall (Weiger *et al.* 2002, Iqbal *et al.* 2004, Riitano 2005, Sathorn *et al.* 2005a), though with variable results.

Experimental fracture studies using extracted teeth are plagued by a wide variability within groups (often a three- or fourfold range in fracture loads), which makes it difficult to demonstrate statistically significant effects of treatment procedures (Lertchirakarn *et al.* 1999, Wu *et al.* 2004, Lam *et al.* 2005, Sathorn *et al.* 2005a). Despite the recognized limitations of numerical methods such as finite element analysis, they offer considerable advantages in the systematic investigation of experimental variables. Even when experimental validation is not possible, carefully constructed models can provide valuable insights into patterns and mechanisms of clinical failure. In this study, a three-dimensional finite element model of a mandibular incisor was constructed to test the effect of canal preparation on stress distributions within the root during compaction. Models with either a round or an oval canal profile were based on measurements from extracted teeth, and were tested for the effects of a canal preparation sequence using either ProTaper or ProFile rotary nickel–titanium instruments (Dentsply Maillefer, Ballaigues, Switzerland). The hypothesis tested in the study was that canal enlargement with instruments of controlled taper would lead to a more uniform stress distribution within the root, and thereby potentially reduce fracture susceptibility.

Materials and methods

Stress distributions in the root of a mandibular right lateral incisor were evaluated for various canal shapes using finite element analysis (MSC.Marc, MSC.Software Corporation, Santa Ana, CA, USA). The three-dimensional external anatomy of the incisor was digitized using an optical scanner (Comet 100, Steinbichler Optical Technologies, Neubeuern, Germany) which generates a point cloud. From this cloud of points, a fine distribution of surface elements was generated using Cumulus software (copyright Regents of the University of Minnesota) (Fig. 1). The geometrical model for the finite element analysis was created using custom software that was specifically developed for automatic generation of internal volumetric element distributions (mesh) within digitized dental anatomies. Since the objective of this study was to evaluate the effect of canal shape on the stress distribution in the root, only the root was meshed (0–12 mm, measured from the apex).

Two basic canal shapes were used for the intact baselines: a round and an oval canal (Fig. 1). The canal sizes were based on measurements performed on cross-sections of extracted teeth. The canal diameter dimensions at 12 mm were 0.20 mm mesial-distal by 0.25 mm buccal-lingual for the round canal, and 0.25 mm mesial-distal by 0.60 mm buccal-lingual for the oval canal. Canal preparations were subsequently created by superimposing the shape of a rotary instrument over the intact canal (Fig. 2), without incorporating any lateral movement that would eliminate the buccal and lingual fins of the oval canal. The file shapes were determined from manufacturer supplied diagrams. Five different files were evaluated: ProTaper F1, F2, F3 and ProFile size 30, 0.04 taper and size 30, 0.06 taper (Dentsply Maillefer), each resulting in a unique canal shape (Fig. 3).

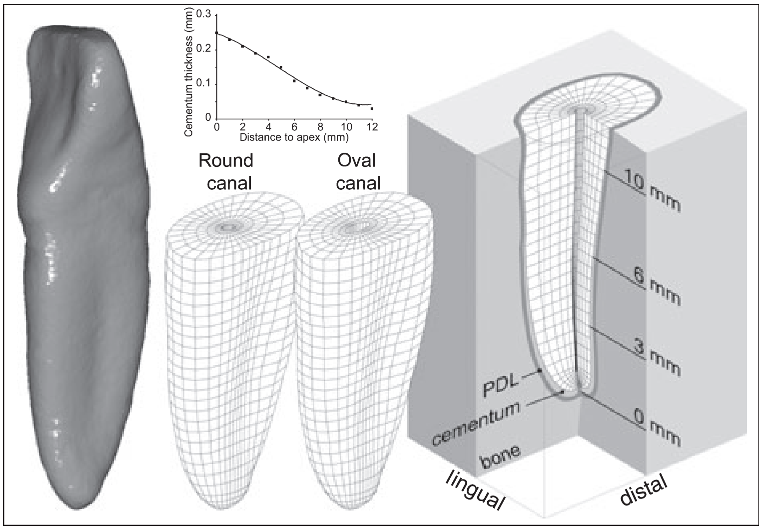

Figure 1 The external anatomy of a mandibular right lateral incisor was digitized. The root was meshed for two canal types (round and oval) and additional layers of cementum, periodontal ligament, and a supporting bone socket were added for the finite element analysis.

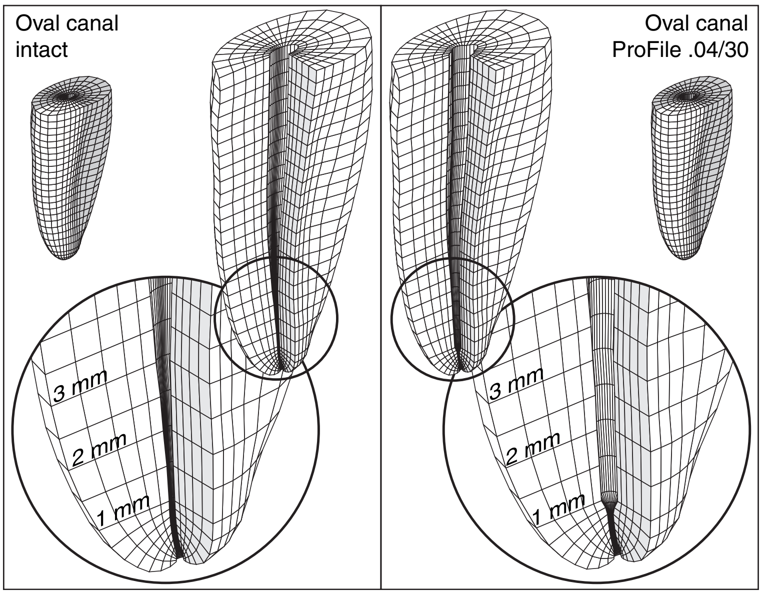

Figure 2 The shape of different rotary instruments were superimposed on the intact canals. Shown are the finite element models of the root for the oval canal before and after preparation with a ProFile 0.04/30 rotary nickel–titanium instrument (Dentsply Maillefer).

The root was covered with a cementum layer, and supported via a simulated periodontal ligament in a bone socket (Fig. 1). The model constraints were achieved by fixing the bone at the bottom. The variation of the cementum thickness along the root surface was based on average cementum thickness values measured on cross-sections of extracted teeth (Fig. 1), whilst its mechanical properties were chosen to be similar to the surrounding bone. The periodontal ligament was modelled as a soft, 200 μm thick,

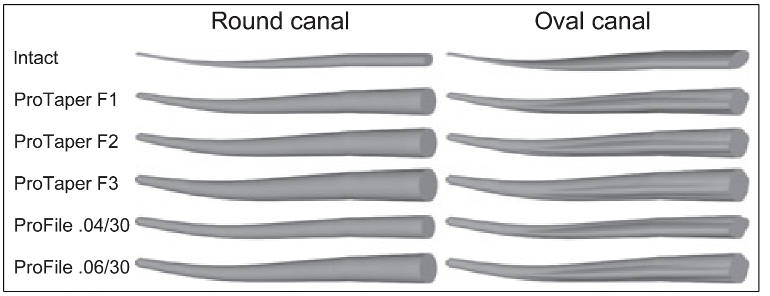

Figure 3 A total of 12 unique canal shapes were created for finite element evaluation after a round or oval canal were superimposed by five different rotary nickel–titanium instruments.

Table 1 Mechanical properties applied in the finite element analysis

	Elastic modulus (GPa)	Poisson's ratio
Dentine	14.7[a]	0.31[b]
Cementum	0.49	0.30
Periodontal ligament	0.00118[c]	0.50
Bone	0.49[d]	0.30[b]

[a]Sano *et al.* (1994); [b]Farah *et al.* (1989); [c]Dyment & Synge (1935); [d]Moroi *et al.* (1993).

incompressible layer. Homogeneous isotropic properties applied in the analysis are listed in Table 1. A uniformly distributed load (50 N mm^{-2}) was applied on the canal wall from 1 to 12 mm (measured from the apex), which simulated lateral pressure during filling.

Results

Root stresses during a simulated compaction procedure were calculated for the two intact baseline canal shapes (round and oval) and for when the canals were prepared with five different rotary instrument sizes. Modified Von Mises equivalent stress distributions are shown along the root surfaces and across various cross-sections (3, 6 and 10 mm) (Fig. 4). The equivalent stress combines the six stress components from the three-dimensional stress state according to a relationship known as the Von Mises criterion. Since dentine strength in tension is approximately three times lower than in compression (Craig & Powers 2002), the Von Mises criterion was modified to account for the fact that tensile stress components are more critical than compressive (de Groot *et al.* 1987, Versluis *et al.* 1997). The equivalent stress distribution for the root with round canal (Fig. 4a) shows the highest stresses at the canal wall, where they are evenly distributed. Increasing the preparation size only marginally affects the stress levels around the round canal wall; however, stress levels at the external distal root surface rose as preparation size increased. The root with oval canal (Fig. 4b) also shows that the highest stress levels are at the canal wall, but the distribution is uneven with high stress concentrations at the buccal and lingual extensions where the radius of curvature is smallest. The stress distribution around the canal at 3 mm was lowered and became uniform when its oval shape was completely rounded by the preparations. A stress concentration also appears at the external distal root surface for the intact oval canal, which was little affected by the subsequent preparations.

Circumferential stresses were determined along the canal surface. A circumferential stress is the stress component in the three-dimensional stress field that is tangentially aligned to the canal surface in the horizontal cross-sectional plane. Figure 5 shows the range of stress values between the maximum (solid lines) and minimum (dashed lines) circumferential stresses along the canal wall for all intact and prepared canals. The circumferential stresses around and along the round canal are uniform, and approximately the same in magnitude for all preparations (Fig. 5a,b). The stresses around the oval canal show a wide range between the maximum and minimum values, indicating high stress concentrations (Fig. 5c,d). Subsequent preparations of the oval canal eliminated the stress concentrations within the apical third where the canal was rounded by the rotary instruments. Where the fins were not completely eliminated in the middle and coronal thirds, the stress levels showed a moderate reduction in stress concentrations.

Discussion

The objective of this study was to evaluate the effect of rotary nickel–titanium canal preparation on root stresses, with the well-accepted assumption that

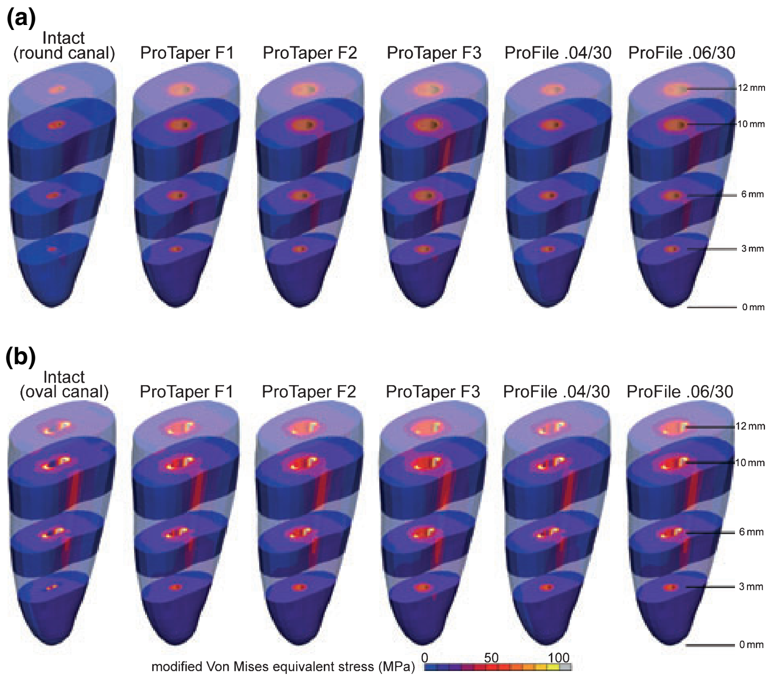

Figure 4 Equivalent stress distributions in a root with (a) a round and (b) an oval canal prepared with five different rotary nickel–titanium instruments when subjected to a uniform wall-pressure of 50 N mm^{-2}.

lowering stress concentrations reduces the risk of vertical root fractures. Fracture can be initiated during compaction or functional loading (Rundquist & Versluis 2006). This study investigated stresses generated during a simulated compaction. Stress values and their distribution throughout the root depend on the root anatomy and loading. The finite element model constructed for this study was based on the external root morphology of a mandibular incisor, and the canal shapes and diameters were based on measurements of 10 incisors. Thus the models created take into account the complexities of real teeth. Although the distribution of stresses will vary amongst teeth according to individual tooth shape and possibly other factors such as age and history of occlusal stresses, the principles of changes in stress distribution reported here should be generally applicable in a clinical situation. The canal preparations superimposed on the model were also clinically realistic, with preparations to a final apical size of 30, and taper of either 0.04, 0.06 (ProFile) or the variable apical size and taper of ProTaper F1–F3. Larger apical sizes are recommended by many practitioners. With these instrument sizes and tapers, the initially round canal was prepared to a smooth, round, tapered preparation throughout its entire length. The oval canal was enlarged to a round shape only in the apical 3–4 mm, and in the middle and coronal one-thirds the canal had a central bulge with uninstrumented fins extending buccally and lingually. This pattern reflects clinical and experimental experience with oval canals (Rödig *et al.* 2002, Weiger *et al.* 2002, Sathorn *et al.* 2005a).

Compaction forces were simulated by a uniform pressure of 50 N mm^{-2} on the canal wall. Regular compaction forces have been reported to be between 10 and 30 N (1–3 kgf) (Harvey *et al.* 1981, Lertchirakarn *et al.* 1999), whilst fracture loads for mandibular roots varied widely between 3 and 88 N (Lertchirakarn *et al.* 1999, 2003, Sathorn *et al.* 2005b). Since the modulus of gutta-percha is low compared with the root and assuming incompressible behaviour, the wall pressure will approximate the pressure applied on the gutta-percha. Depending on the diameter of the application area, a wall pressure of 50 N mm^{-2} corresponds with 20–40 N compaction force. Thus, the pressure applied in this study was within a clinically relevant range. Besides morphology and loading, mechanical properties also affect the stress conditions. This analysis used values reported in the dental literature (Table 1). It is important to note that although natural variation in

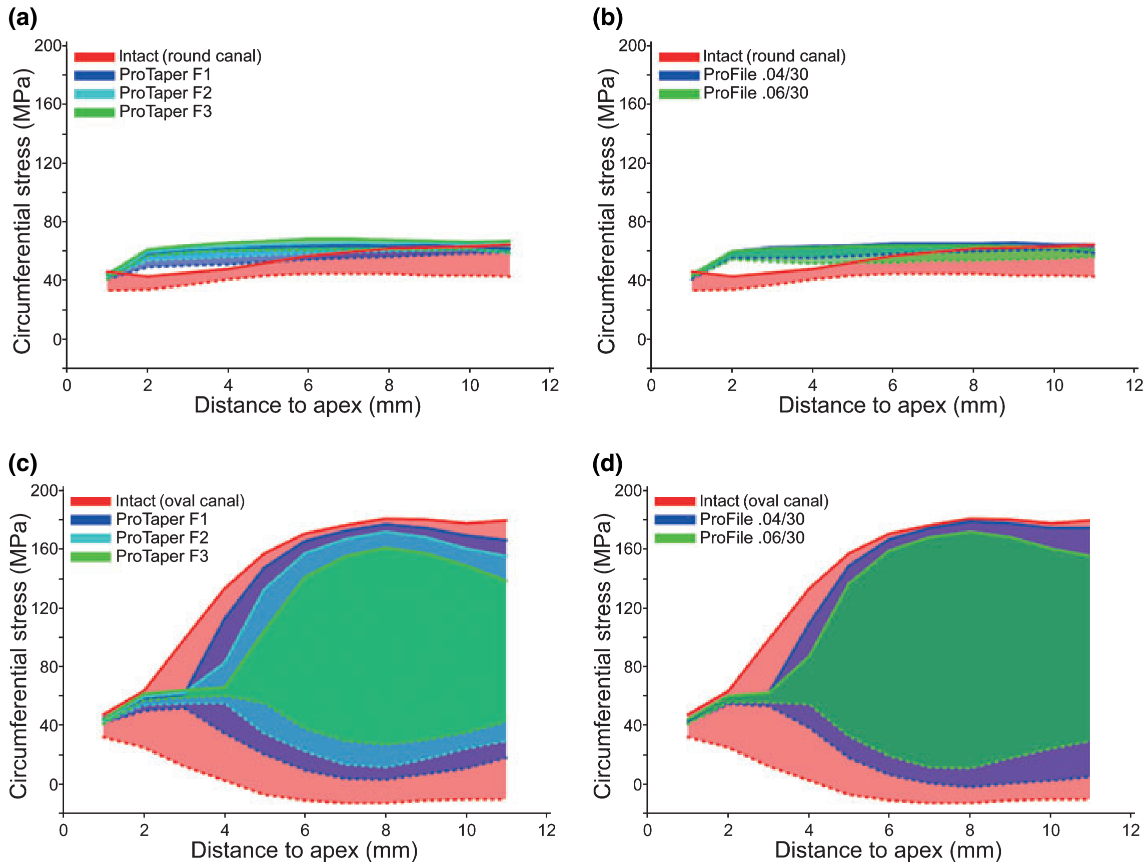

Figure 5 Circumferential stress ranges along the canal wall surface for a root with a round (a, b) and oval canal (c, d), prepared with five different rotary nickel–titanium instruments when subjected to a uniform wall-pressure of 50 N mm^{-2}.

tooth morphology and tissue properties precludes a unique solution, stress calculations can still be validated by verifying that the predicted mechanical response corresponds with experimental observations. In a previous study, circumferential deformation at the external root surface was measured using strain gauges placed between the apical and middle third of resected mandibular incisors (Lertchirakarn *et al.* 2003). Reported circumferential strains (mean ± SD) at 62–88 N fracture loads were −402 ± 218, −1042 ± 1601, 1626 ± 1304 and 3440 ± 4692 μstrain for the buccal, lingual, mesial and distal sites, respectively. For comparison, Table 2 lists the strain values at the dentine–cementum interface calculated in this finite element analysis. Despite the wide variation found in the experimental results, the finite element analysis computed a similar trend where the lowest strains were found at the buccal and lingual sides, and the highest strains were found distally. Furthermore, consistent with the experimental data, the finite element analysis indicated compressive strains at the buccal and lingual surfaces and tensile strains at the mesial and distal surfaces. When the differences in compaction forces were taken into account, the calculated strains were within the same order of magnitude as found in the experiments.

The finite element results indicated that when an internal load was applied in models with a round canal, the stress distribution was low and relatively uniform both around the canal wall and from apical to coronal (Fig. 4a). The thickness of the surrounding root dentine hardly affected this distribution. In contrast, the oval canal showed much higher stresses and a very uneven stress distribution, both around the canal wall and from apical to coronal (Fig. 4b). Stresses were concentrated at the buccal and lingual canal extensions (location of sharpest canal concavities), and increased threefold from the apical 1 mm to the coronal one-half of the

Table 2 Circumferential strains (μstrain) at the external root surface (dentine–cementum interface) between the apical and middle third (4 mm from the apex) when the root is subjected to a uniform wall-pressure of 50 N mm^{-2}

	Round canal				Oval canal			
	Buccal	Lingual	Mesial	Distal	Buccal	Lingual	Mesial	Distal
Intact	−13	−10	58	179	−67	−75	359	855
ProTaper F1	−48	−38	231	718	−73	−73	356	950
ProTaper F2	−65	−53	344	1038	−81	−75	404	1138
ProTaper F3	−85	−68	481	1427	−93	−81	505	1461
ProFile 0.04/30	−41	−32	241	722	−69	−69	365	960
ProFile 0.06/30	−62	−48	328	1003	−79	−72	399	1121

Negative strain values indicate compression, positive values denote tension.

canal. The stress distributions are consistent with those reported previously (Lertchirakarn *et al.* 2003, Sathorn *et al.* 2005a), based on simpler geometric models. Stress concentrations were eliminated in the areas where the sharp edges of the oval canal were completely smoothed out by the rotary instruments (see the 3 mm cross-sections in Fig. 4b).

Comparatively moderate stress concentrations (less than half of the stress levels calculated along the canal surface) were found at the mesial and distal middle and coronal one-thirds of the proximal external surfaces of the roots with oval canals (Fig. 4b). Preparations with different rotary instrument sizes minimally affected the magnitude of these stress concentrations. In contrast, the root with the intact round canal showed very little distal and mesial stress elevation at its root surfaces (Fig. 4a). However, its external root surface stress levels increased with increasing rotary instrument diameters, where preparation with the largest instrument (ProTaper F3) approached the surface stress conditions found for the root with an oval canal. The observed stress distributions suggest that the bucco-lingual dimension of the canal space may be a determining factor for the extent of distal and mesial proximal surface stresses.

Consistent with previous reports in the literature (Lertchirakarn *et al.* 2003, Sathorn *et al.* 2005a, Rundquist & Versluis 2006), the finite element analysis indicated that the highest stresses during simulated internal compaction loading were not found at the external root surface, but at the canal wall (Fig. 4). Therefore, the most clinically significant results from the current stress analysis are the circumferential stresses. Preparation of round canals led to only small increases in circumferential stresses in the apical half (Fig. 5a,b), with potentially only modest changes in fracture susceptibility of the root. The maximum stress values remained approximately the same after preparation with all instrument sizes, albeit the maximum circumferential stress values that were originally confined to the coronal one-third spread over almost the entire canal length. The stress distribution was also more uniform around the canal wall, illustrated by the close values of the maximum and minimum stresses (narrow bands) compared with the oval canals (Fig. 5c,d). Large differences between the maximum and minimum circumferential stress values (wide bands) were found for the oval canals, confirming the differences in equivalent stress concentrations between the two canal types observed earlier (Fig. 4). In contrast to the round canal, preparation of the oval canal led to substantial reduction in circumferential stresses at the canal wall (Fig. 5c,d), particularly in the apical one-third where the canal was enlarged to a smooth round shape. Interestingly, in the middle and coronal thirds, where the buccal and lingual fins were not completely eliminated, the maximum stresses were still reduced by up to 15% (with ProTaper F3). Thus, even though the effect was relatively small when the fins were not contacted by the instrument, the stresses within the root were lower and more evenly distributed than in the intact root before canal preparation. A fully round preparation, such as was achieved in the apical one-third, led to a much greater reduction in stress even in comparison with the uninstrumented canal. If these results can be extrapolated to the clinical situation, the potential for reducing fracture susceptibility exists as a result of the round canal profiles achieved and the smooth canal taper. Previous experimental studies using extracted teeth have reported only small effects of canal preparation on fracture resistance relative to uninstrumented controls (Cobankara *et al.* 2002, Wu *et al.* 2004, Zandbiglari *et al.* 2006); results have varied depending on tooth type, method of canal preparation and loading system and have been characterized by large variability amongst teeth.

Conclusions

1. The largest stresses during an internal compaction load for a mandibular incisor occurred at the canal wall surface. Where round canals exhibited an even distribution, oval canals caused high stress concentrations at the buccal and lingual canal extensions.

2. Creating a fully round preparation reduced stress concentrations. Even when fins were not completely smoothed by the instruments, the stresses within the root were reduced by up to 15% and more evenly distributed than in the intact root before canal preparation.

3. The potential for reducing fracture susceptibility with nickel–titanium instruments exists as a result of the round canal profiles achieved and the smooth canal taper.

Acknowledgements

This study was supported in part by the Minnesota Dental Research Center for Biomaterials and Biomechanics. The authors also thank Dr D. Tantbirojn for her advice.

References

Bryant ST, Thompson SA, al-Omari MAO, Dummer PMH (1998) Shaping ability of profile rotary nickel–titanium instruments with ISO sized tips in simulated root canals: part 1. *International Endodontic Journal* **31**, 275–81.

Caplan DJ, Weintraub JA (1997) Factors related to loss of root canal filled teeth. *Journal of Public Health Dentistry* **57**, 31–9.

Cobankara FK, Ungor M, Belli S (2002) The effect of two different root canal sealers and smear layer on resistance to root fracture. *Journal of Endodontics* **28**, 606–9.

Craig RG, Powers JM (2002) *Restorative Dental Materials*, 11th edn. St Louis, MO: Mosby.

Dyment MI, Synge JL (1935) The elasticity of the periodontal membrane. *Oral Health* **25**, 105–9.

Farah JW, Craig RG, Meroueh KA (1989) Finite element analysis of three- and four-unit bridges. *Journal of Oral Rehabilitation* **16**, 603–11.

Fuss Z, Lustig J, Tamse A (1999) Prevalence of vertical root fractures in extracted endodontically treated teeth. *International Endodontic Journal* **32**, 283–6.

Glosson CR, Haller RH, Dove SB, del Rio CE (1995) A comparison of root canal preparations using Ni–Ti hand, Ni–Ti engine-driven, and K-Flex endodontic instruments. *Journal of Endodontics* **21**, 146–51.

de Groot R, Peters MCRB, de Haan YM, Dop GJ, Plasschaert AJM (1987) Failure stress criteria for composite resin. *Journal of Dental Research* **66**, 1748–52.

Harvey TE, White JT, Leeb IJ (1981) Lateral condensation stress in root canals. *Journal of Endodontics* **7**, 151–5.

Iqbal MK, Karabucak B, Brown M, Menegazzo E (2004) Effect of modified Hedstrom files on instrumentation area produced by ProFile instruments in oval canals. *Oral Surgery, Oral Medicine, Oral Pathology* **98**, 493–8.

Lam PP, Palamara JEA, Messer HH (2005) Fracture strength of tooth roots following canal preparation by hand and rotary instrumentation. *Journal of Endodontics* **31**, 529–32.

Lertchirakarn V, Palamara JEA, Messer HH (1999) Load and strain during lateral condensation and vertical root fracture. *Journal of Endodontics* **25**, 99–104.

Lertchirakarn V, Palamara JEA, Messer HH (2003) Finite element analysis and strain-gauge studies of vertical root fracture. *Journal of Endodontics* **29**, 529–34.

Lindauer PA, Campbell AD, Hicks ML, Pelleu GB (1989) Vertical root fractures in curved roots under simulated clinical conditions. *Journal of Endodontics* **15**, 345–9.

Moroi HH, Okimoto K, Moroi R, Terada Y (1993) Numeric approach to the biomechanical analysis of thermal effects in coated implants. *International Journal of Prosthodontics* **6**, 564–72.

Peters OA (2004) Current challenges and concepts in the preparation of root canal systems: a review. *Journal of Endodontics* **30**, 559–67.

Riitano F (2005) Anatomic endodontic technology (AET) – a crown-down root canal preparation technique: basic concepts, operative procedure and instruments. *International Endodontic Journal* **38**, 575–87.

Rödig T, Hülsmann M, Mühge M, Schäfers F (2002) Quality of preparation of oval distal root canals in mandibular molars using nickel–titanium instruments. *International Endodontic Journal* **35**, 919–28.

Rundquist BD, Versluis A (2006) How does canal taper affect root stresses? *International Endodontic Journal* **39**, 226–37.

Sano H, Ciucchi B, Matthews WG, Pashley DH (1994) Tensile properties of mineralized and demineralized human and bovine dentin. *Journal of Dental Research* **73**, 1205–11.

Sathorn C, Palamara JEA, Messer HH (2005a) A comparison of the effects of two canal preparation techniques on root fracture susceptibility and fracture pattern. *Journal of Endodontics* **31**, 283–7.

Sathorn C, Palamara JEA, Palamara D, Messer HH (2005b) Effect of root canal size and external root surface morphology on fracture susceptibility and pattern: a finite element analysis. *Journal of Endodontics* **31**, 288–92.

Sedgley CM, Messer HH (1992) Are endodontically treated teeth more brittle? *Journal of Endodontics* **18**, 332–5.

Teixeira FB, Teixeira ECN, Thompson JY, Trope M (2004) Fracture resistance of roots endodontically treated with a new resin filling material. *Journal of the American Dental Association* **135**, 646–52.

Thompson SA, Dummer PMH (1997) Shaping ability of ProFile .04 Taper Series 29 rotary nickel-titanium instruments in simulated root canals. Part 1. *International Endodontic Journal* **30**, 1–7.

Versluis A, Tantbirojn D, Douglas WH (1997) Why do shear bond tests pull out dentin? *Journal of Dental Research* **76**, 1298–307.

Weiger R, ElAyouti A, Löst C (2002) Efficiency of hand and rotary instruments in shaping oval root canals. *Journal of Endodontics* **28**, 580–3.

Wilcox LR, Roskelley C, Sutton T (1997) The relationship of root canal enlargement to finger-spreader induced vertical root fracture. *Journal of Endodontics* **23**, 533–4.

Wu M-K, R'oris A, Barkis D, Wesselink PR (2000) Prevalence and extent of long oval canals in the apical third. *Oral Surgery, Oral Medicine, Oral Pathology, Oral Radiology and Endodontics* **89**, 739–43.

Wu M-K, van der Sluis LWM, Wesselink PR (2004) Comparison of mandibular premolars and canines with respect to their resistance to vertical root fracture. *Journal of Dentistry* **32**, 265–8.

Zandbiglari T, Davids H, Schäfer E (2006) Influence of instrument taper on the resistance to fracture of endodontically treated roots. *Oral Surgery, Oral Medicine, Oral Pathology, Oral Radiology and Endodontics* **101**, 126–31.